



HAL
open science

Cumulative air density depletion during high repetition rate filamentation of femtosecond laser pulses: Application to electric discharge triggering

Pierre Walch, Benoît Mahieu, Leonid Arantchouk, Yves-Bernard André,
André Mysyrowicz, Aurélien Houard

► To cite this version:

Pierre Walch, Benoît Mahieu, Leonid Arantchouk, Yves-Bernard André, André Mysyrowicz, et al.. Cumulative air density depletion during high repetition rate filamentation of femtosecond laser pulses: Application to electric discharge triggering. Applied Physics Letters, 2021, 119 (26), pp.262101. 10.1063/5.0077635 . hal-03510763

HAL Id: hal-03510763

<https://ensta-paris.hal.science/hal-03510763v1>

Submitted on 4 Jan 2022

HAL is a multi-disciplinary open access archive for the deposit and dissemination of scientific research documents, whether they are published or not. The documents may come from teaching and research institutions in France or abroad, or from public or private research centers.

L'archive ouverte pluridisciplinaire **HAL**, est destinée au dépôt et à la diffusion de documents scientifiques de niveau recherche, publiés ou non, émanant des établissements d'enseignement et de recherche français ou étrangers, des laboratoires publics ou privés.



Distributed under a Creative Commons Attribution 4.0 International License

Cumulative air density depletion during high repetition rate filamentation of femtosecond laser pulses: Application to electric discharge triggering

Cite as: Appl. Phys. Lett. **119**, 264101 (2021); <https://doi.org/10.1063/5.0077635>

Submitted: 04 November 2021 • Accepted: 10 December 2021 • Published Online: 27 December 2021

 P. Walch,  B. Mahieu,  L. Arantchouk, et al.



View Online



Export Citation



CrossMark

ARTICLES YOU MAY BE INTERESTED IN

[Measurement matrix uncertainty model-based microwave induced thermoacoustic sparse reconstruction in acoustically heterogeneous media](#)

Applied Physics Letters **119**, 263701 (2021); <https://doi.org/10.1063/5.0076449>

[p-type c-Si/SnO₂/Mg heterojunction solar cells with an induced inversion layer](#)

Applied Physics Letters **119**, 263502 (2021); <https://doi.org/10.1063/5.0070585>

[Atomically thin In₂O₃ field-effect transistors with 10¹⁷ current on/off ratio](#)

Applied Physics Letters **119**, 263503 (2021); <https://doi.org/10.1063/5.0075166>

 QBLOX



1 qubit

Shorten Setup Time

Auto-Calibration
More Qubits

Fully-integrated

Quantum Control Stacks
Ultrastable DC to 18.5 GHz
Synchronized <<1 ns
Ultralow noise



100s qubits

[visit our website >](#)



Cumulative air density depletion during high repetition rate filamentation of femtosecond laser pulses: Application to electric discharge triggering

Cite as: Appl. Phys. Lett. **119**, 264101 (2021); doi: [10.1063/5.0077635](https://doi.org/10.1063/5.0077635)

Submitted: 4 November 2021 · Accepted: 10 December 2021 ·

Published Online: 27 December 2021



View Online



Export Citation



CrossMark

P. Walch,^{a)} B. Mahieu, L. Arantchouk, Y.-B. André, A. Mysyrowicz, and A. Houard

AFFILIATIONS

LOA, ENSTA Paris, CNRS, École Polytechnique, Institut Polytechnique de Paris, 828 Bd des Maréchaux, 91762 Palaiseau, France

^{a)} Author to whom correspondence should be addressed: pierre.walch@ensta-paris.fr

ABSTRACT

We study the influence of the laser repetition rate on the generation of low-density channels of air left in the path of femtosecond laser filamentation. At high repetition rates, we observe the formation of a permanent millimeter-wide low-density channel that exceeds the depth and width of the transient depletion due to a single filament. We also show that this permanent cumulative effect decreases the breakdown voltage between two electrodes and can alter the path of the discharge. By comparing this effect in air and in pure nitrogen, we show that an accumulation of O_2^- ions contributes to the reduction in the breakdown voltage.

© 2021 Author(s). All article content, except where otherwise noted, is licensed under a Creative Commons Attribution (CC BY) license (<http://creativecommons.org/licenses/by/4.0/>). <https://doi.org/10.1063/5.0077635>

The propagation of intense short laser pulses in atmosphere gives rise to a filamentation process during which a core of the pulse maintains a high peak intensity over distances exceeding by far the Rayleigh length, as if diffraction was suppressed. Due to the high laser intensity of this core, high field ionization occurs, and consequently, a plasma column is formed in the wake of the propagating elementary pulse, opening the possibility for many applications.^{1,2} One such application is the triggering and guiding of atmospheric discharges.^{3–9} Following the development of terawatt lasers operating at high repetition rates, growing attention is devoted to the study of the filament process and to the guiding of electric discharges at such high repetition rates.^{10–15} In this article, we study the influence of the laser repetition rate on the production of low-density channels of air formed in the path of the filament plasma by the sudden laser energy absorption and on the guiding of electric discharges.

This article is organized as follows. We first analyze the temporal evolution of the under-dense air channel produced by filamentation in a single laser pulse regime and compare it to simulation. We then measure the under-dense channels occurring with a laser operating at variable repetition rates between 10 and 1 kHz and compare them with simulations at the same repetition rates. The impact of a steady air flow at different air velocities is then studied numerically and experimentally. Finally, we measure the effect these accumulations have on the breakdown voltage of a cm-scale high voltage discharge and show that it can modify the trajectory of these discharges.

To model the evolution of the under-dense air channel,^{12,15,16} we consider the air thermodynamics occurring after the under-dense channel has reached pressure equilibrium with the ambient air at temperature T_{amb} . Its maximum depth and peak temperature slowly decay on a millisecond timescale because of thermal diffusion. Outside from the edges, the under-dense channel can be considered approximately invariant along the channel axis z . Its temporal evolution can then be modeled as $T(x, y, t) = T_{amb} + \Delta T(x, y, t)$ with

$$\Delta T(x, y, t) = \Delta T_0 \times R_0^2 / (\sqrt{R_0^2 + 4 \times \alpha \times t})^2 \times e^{-\frac{x^2 + (y-v(t) \times t)^2}{(\sqrt{R_0^2 + 4 \times \alpha \times t})^2}},$$

where α is the thermal diffusivity of air,¹⁷ T_{amb} is the room temperature, R_0 and ΔT_0 are, respectively, the radius and the peak temperature change of the initial Gaussian temperature distribution,¹² x and y are, respectively, the position on the horizontal and vertical axis, centered on the channel axis z , and v is the speed at which the channel moves upward. It consists of the buoyant force and a corrective term $v_{airflow}$ to take into account any additional air flow in the study zone

$$v(t) = \left(1 - \frac{T_{amb} + \Delta T_0}{T_{amb}}\right) \times g \times t + v_{airflow}, \quad (1)$$

where g is the acceleration of gravity. As pressure equilibrium is maintained during the studied phase of the evolution, the relation between the density and temperature change is $\Delta n/n_{amb} = -\Delta T/T_{amb}$, where

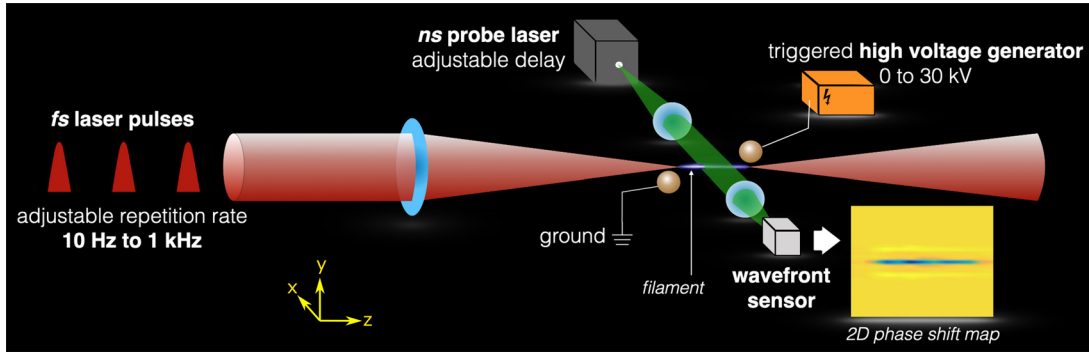


FIG. 1. Experimental setup. A mJ-level femtosecond laser pulse sequence of 800-nm central wavelength and 50 fs duration is focused in air and creates a 1 cm-long filament. The repetition rate of the femtosecond laser is tuned from 10 Hz to 1 kHz. The resulting low air-density channel is probed by a nanosecond laser beam coupled to a Phasics SID4 wavefront sensor, which records a two-dimensional phase shift map. For discharge guiding measurements, two spherical electrodes of radius 6 mm separated by 8 mm are placed at the filament edges and connected to a pulsed high-voltage generator.

n_{amb} is the ambient air density. This density variation is measured with the setup presented in Fig. 1. The recorded phase shift can be linked to the density variation by

$$\Delta\phi = \frac{2\pi\beta}{\lambda} \int \frac{\Delta n(s)}{n_{amb}} ds, \quad (2)$$

where β is the Gladstone–Dale constant.

To test the validity of this air thermodynamics model, we compare its prediction with measurements of the under-dense channel resulting from the filamentation of a single 14 mJ, 50 fs laser pulse at 800 nm focused at $f/33$. This comparison is presented in Fig. 2 at delays with respect to the fs laser pulse ranging between 5 μ s and 3500 μ s with the input parameters $\Delta T_0 = 700$ K and $R_0 = 170$ μ m. A satisfactory agreement is found between the simulation and measurements. The temperature and radius variations are in the range of previous measurements.¹⁶

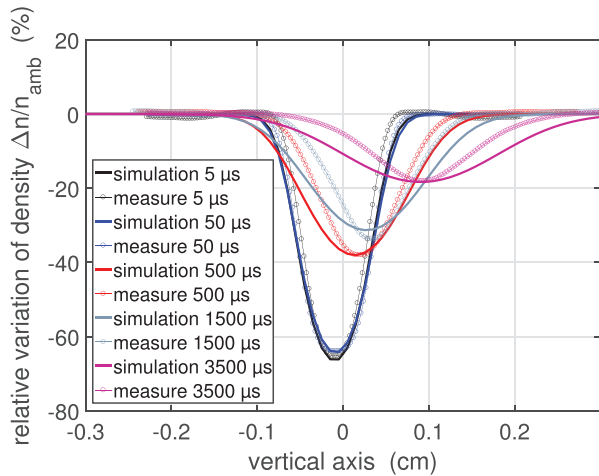


FIG. 2. Circles: Measured temporal evolution of the density variation profile along the y axis resulting from the filamentation of 14 mJ, 50 fs laser pulses focused at $f/33$. Full line: simulated temporal evolution of the same profile with input parameters $\Delta T_0 = 700$ K and $R_0 = 170$ μ m.

Using the same model, we now analyze the thermally induced changes of density resulting from filamentation at high laser repetition rates. Considering a train of n pulse from a laser set at a repetition rate f , the total thermal variation $\Delta T_{cumul}(x, y, t)$ can be expressed as

$$\Delta T_{cumul}(x, y, t) = \sum_{i=0}^{n-1} \Delta T \left(x, y, t + \frac{i}{f} \right). \quad (3)$$

Note that this expression can only be used for small temperature variations ($\Delta T < 300$ K). For higher temperature changes, effects, such as the interaction of an incoming pulse with the previously formed channel, should be taken into account. In Fig. 3(a), the phase shift induced by filamentation of a 0.8 mJ, 50 fs laser pulse at 800 nm, focused at $f/100$, measured at different repetition rates, is presented together with the simulated phase shift using the input parameters $\Delta T_0 = 18$ K and $R_0 = 170$ μ m. The delay between the last laser pulse and the observation time is set at 100 s to ensure that the shockwave induced by the last laser pulse has exited the studied zone. A clear accumulation effect can be seen starting at 100 Hz and increasing at higher repetition rates. The simulated phase shifts show good agreement with the measurements. The observed asymmetry is due to the upward motion of the individual under-dense channels due to buoyancy. This asymmetry causes a downward deflection of the laser path itself that we also observe after the filamentary zone, see Figs. 4(b)–4(e).¹² One important aspect of this cumulative effect is its longevity. At repetition rates higher than 100 Hz, the delay that separates each pulse is shorter than the lifetime of each individual under-dense channel. As a consequence, the under-dense channel remains during the whole laser operation. The channel consists then in two parts: One that evolves over a millisecond timescale due to heating by the last laser shot and a second one due to the accumulation of the previous laser heating that remains constant between each laser pulse. Evidence for these two parts of the channel evolution is shown in Fig. 3(b), where the measurements are made at different delays from the last laser pulse. The fast evolution that is generated by the last laser pulse can be seen on the measurement made at a delay of 100 μ s but is not seen at the delay of 9990 μ s, because it has already fully merged within the accumulated heating. The second part is constant in the three measurements, proving its longevity.

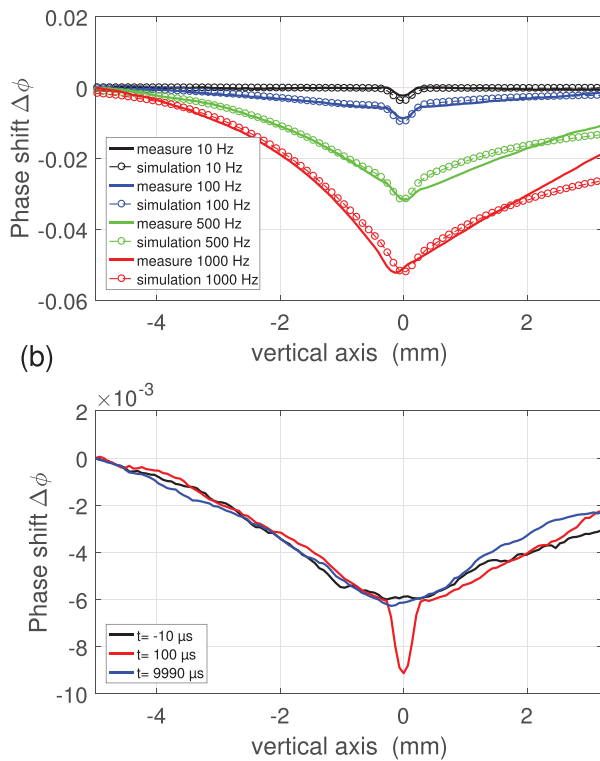


FIG. 3. Phase shifts induced by the filamentation of 0.8 mJ, 35 fs laser pulses focused at $f/100$. (a) Phase shifts measured 100 μs after the last laser pulse (full line) and corresponding simulations (circles) at various repetition rates. (b) Phase shifts measured at different delays after the last laser pulse at a 100 Hz repetition rate.

The cumulative effects, being strongly related to air dynamics, should be sensitive to a change in the air flow. To verify this effect, we measured the phase shift induced from the previously described laser operating at a repetition rate of 1000 Hz in the presence of a steady air flow of the variable speed created by a fan blowing upward. The results shown in Fig. 4(a) are compared with the simulated phase shift calculated with an appropriate value v_{airflow} . As v_{airflow} increases, the accumulation effect is greatly reduced. At 1000 Hz, the cumulative effect has completely disappeared with $v_{\text{airflow}} = 3.5 \text{ m s}^{-1}$. The same experiment, repeated at a repetition rate of 500 Hz, shows that the cumulative effect already disappears at $v_{\text{airflow}} = 0.8 \text{ m s}^{-1}$. This indicates that the air flow required to remove the cumulative effect decreases as the laser repetition rate is decreased.

Femtosecond filaments have proved to be a powerful tool to trigger and guide electric discharges in atmosphere. The formation of a low density channel by the filament is the main mechanism responsible for this guiding effect.^{16,18,19} The density decrease in the channel lowers the breakdown voltage between two charged electrodes, forming a preferential path for the discharge. Other filament effects that can also influence the discharge propagation are the presence of long lived free electrons²⁰ or electrons loosely attached to oxygen molecules that are generated during the plasma recombination.^{3,21} One, therefore, expects that the filament cumulative effect reduces the breakdown voltage between the two electrodes. Since the part of the channel

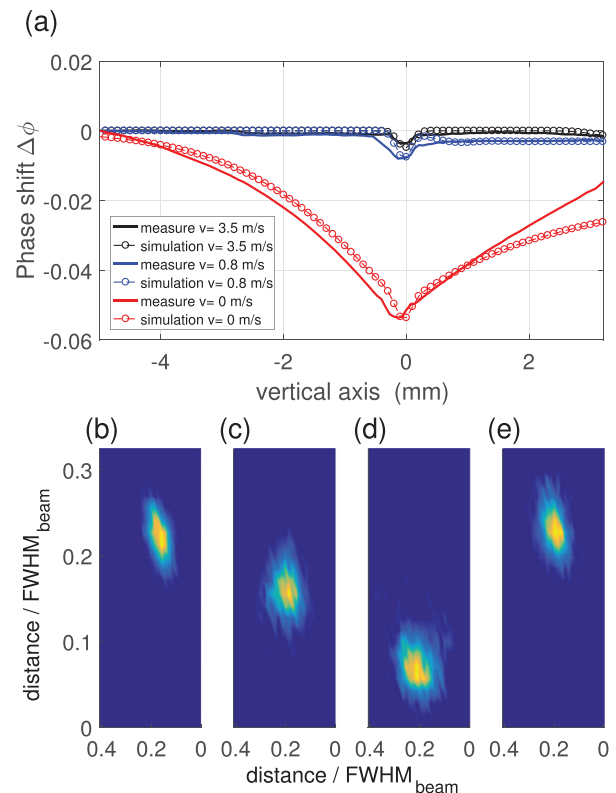


FIG. 4. Effect of a steady air flow on the air channel, with same laser parameters as in Fig. 3. (a) Phase shifts measured (full line) and simulated (circles) with different air flows at a 1000 Hz repetition rate. Input parameters for simulations are $\Delta T_0 = 18 \text{ K}$ and $R_0 = 170 \mu\text{m}$. Downward shift of the mean position of the laser beam after crossing the filamentary zone measured without air flow at 10 (b), 100 (c), 1000 Hz (d), and at 1000 Hz with air flow (e).

resulting from the cumulative effect is constant, one expects a reduction in the breakdown voltage that is constant over time. This removes the need of precise synchronization between the laser pulse and a pulsed high voltage generator.²²

We investigated this concept by triggering spark discharges with a system composed of a high-voltage pulsed generator and two spherical electrodes placed in the vicinity of the filament, as depicted in Fig. 1. The high-voltage generator could deliver single-shot pulses with 5 ns nanosecond duration, a maximum amplitude of 30 kV. Each voltage value was measured with a precision of 2%. The breakdown voltage U_{BD} was defined as the voltage for which a breakdown probability of 100% was obtained over ten shots. The voltage pulse could be advanced with respect to the laser pulse. Figure 5 presents the measured breakdown voltage as a function of the delay between the high voltage pulse and the last laser pulse at different repetition rates. The evolution of the breakdown voltage can be split into two parts: the first one evolving fast over a μs timescale is linked to the quick evolution of the under-dense region. The second one, produced by the cumulative effect, is quasi-constant over the studied timescale of 200 μs . As expected, this second part leads to a reduced breakdown voltage as the repetition rate of the laser is increased.²³

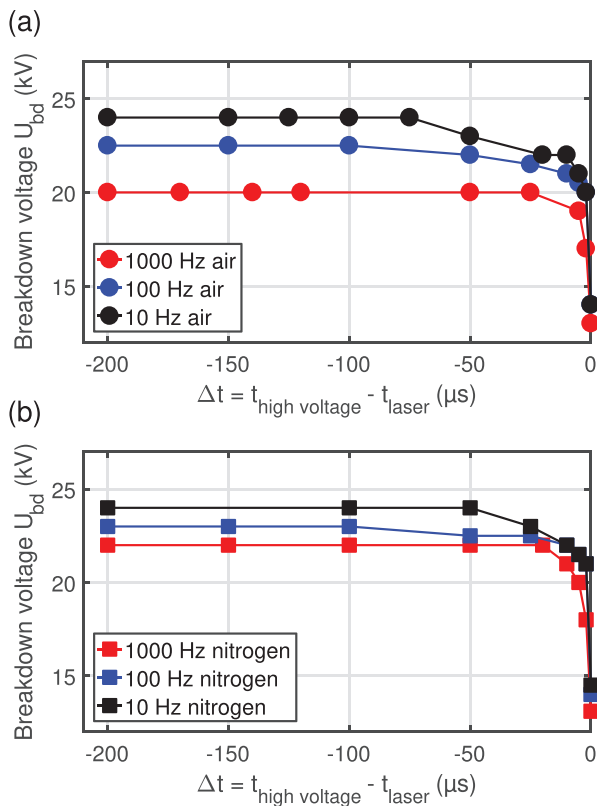


FIG. 5. Breakdown voltage measured with 0.8 mJ, 35 fs laser pulses focused at $f/100$ as a function of the delay between the high voltage generator and the last laser pulse at different laser repetition rates. (a) Measurements made in ambient air. (b) Same measurements made in nitrogen. In both cases, the natural breakdown without lasers is 29 kV.

TABLE I. Table comparing the expected breakdown voltage with the measurement made in air and in nitrogen at a delay of $-100 \mu\text{s}$ for the different laser repetition rates.

Repetition rate (Hz)	ΔT_{max} (K)	Expected V_{bd} (kV)	Measured V_{bd} in air (kV)	Measured V_{bd} in nitrogen (kV)
1000	95	21.9	20.0	22.0
100	71	23.4	22.5	23.0
10	61	24.0	24.0	24.0

Using the air dynamics model, we calculated the thermal variation ΔT_{max} and the theoretical breakdown voltage V_{bd} for each repetition rate and compared it with the measurements. These values are presented in Table I. We note that the measurements made in pure nitrogen match well the theoretical values for the reduced breakdown voltage. However, the measured breakdown field in air is lower than the expected value for 100 Hz and 1 kHz. Considering that ionization and laser energy deposition in the filament are almost the same in air and in nitrogen,¹ the same breakdown field should be observed if the filament hydrodynamic was the only guiding mechanism. We attribute this discrepancy to the presence of long-lived O_2^- ions at high laser repetition rates. These ions provide a reserve of easily detached electrons that facilitate the electrical breakdown. Due to their long lifetime, they can be accumulated at high repetition rates and contribute to the cumulative effect by reducing even further the breakdown voltage.²¹

Finally, a camera picture of the filament region is shown in Fig. 6(a), and pictures of the discharge path are presented in Figs. 6(b)–6(g) for three different delays between the laser and the high-voltage pulse, made with a laser repetition rate of 1 kHz. At a delay of $-2 \mu\text{s}$, the discharge is clearly guided along the laser path. As the delay increases, the distance over which the discharge follows the laser path is reduced. At short delays, the discharges are indeed still

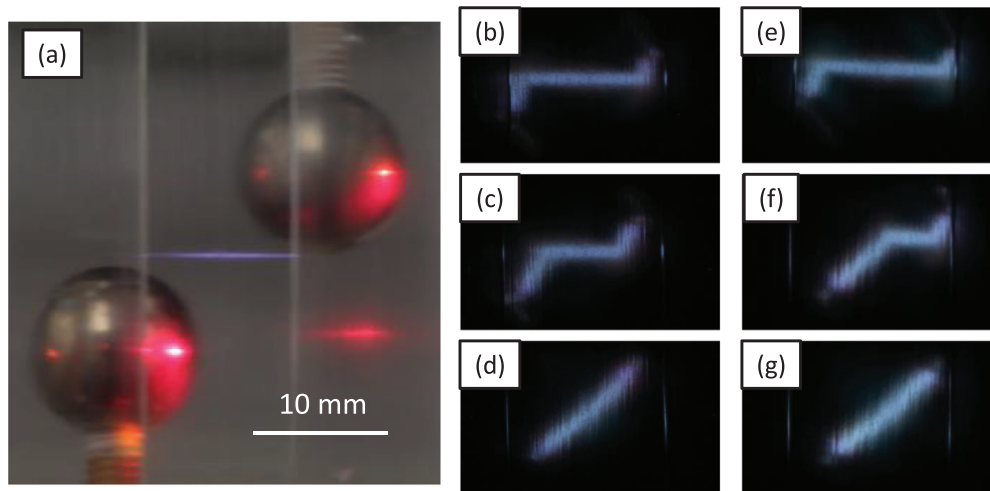


FIG. 6. Pictures of the filament region showing the plasma luminescence and the two electrodes (a). Pictures of the discharge in air for three different triggering times of the high voltage generator with respect to the femtosecond laser pulse arrival time: -2 (b), -25 (c), and $-100 \mu\text{s}$ (d). Pictures of the discharge in pure nitrogen for the same triggering times: -2 (e), -25 (f), and $-100 \mu\text{s}$ (g).

affected by the spatial perturbation made by the last laser pulse. At longer delays, the only remaining perturbation is the one resulting from the cumulative effect. The latter, being spatially wider than the distance between the electrodes, helps the triggering of the discharge without imposing a specific path. The discharge path is then determined by the electric field lines imposed by our setup, as it is the case in regular discharges. The similarity of the discharge paths when they are realized in air or in nitrogen shows that the accumulation of both the heating and the O_2^- ions occurs on a similar spatial scale.

In these experiments, we investigated the influence of a high repetition rate laser on the formation of cm long electric discharges. We note that it should be scalable to longer discharges and even to the guiding of lightning by powerful high repetition rate laser systems.¹¹ Indeed, the laser induced depletion of the air density responsible for the discharge triggering is permanent and, therefore, does not depend on the presence of a plasma of long duration. We also note that the presence of O_2^- ions should facilitate the propagation of lightning precursors called leaders.²⁴

We have shown that an important permanent depletion of air occurs during filamentation of femtosecond pulses at high laser repetition rates. At a kHz laser repetition rate, the depth and width of the low density channel exceeds largely the depth and width created by a single filament. This effect impacts measurements that depend on the gas density. For example, we have shown that it lowers the breakdown voltage of a filament guided electric discharge and can alter its path. By comparing the measurements in air and pure nitrogen, we have shown that long-lived O_2^- ions contribute to further increase this permanent reduction of the breakdown voltage. This permanent reduction could prove useful in applications, where a precise synchronization between the laser and the onset of the HV pulse is not possible such as in a Laser lightning rod.^{11,25}

The authors acknowledge the European Union Horizon 2020 Research and innovation programme FET-OPEN under Grant No 737033-LLR and the French DGA under Grant No. 2018950901 EPAT3. We also acknowledge technical support from Amar Tafzi.

AUTHOR DECLARATIONS

Conflict of Interest

The authors have no conflict of interest to disclose.

DATA AVAILABILITY

The data that support the findings of this study are available from the corresponding author upon reasonable request.

REFERENCES

- A. Couairon and A. Mysyrowicz, "Femtosecond filamentation in transparent media," *Phys. Rep.* **441**, 47–189 (2007).
- Light Filaments: Structures, Challenges and Applications*, edited by L. A. J.-C. Diels and M. C. Richardson (Institution Of Engineering And Technology, 2021).
- X. M. Zhao, J. C. Diels, C. Y. Wang, and J. Elizondo, "Femtosecond ultraviolet laser pulse induced lightning discharges in gases," *IEEE J. Quantum Electron* **31**, 599 (1995).
- D. Comtois, C. Y. Chien, A. Desparois, F. Génin, G. Jarry, T. W. Johnston, J.-C. Kieffer, B. La Fontaine, F. Martin, R. Mawassi, H. Pépin, F. A. M. Rizk, F. Vidal, P. Couture, H. P. Mercure, C. Potvin, A. Bondiou-Clergerie, and I. Gallimberti, "Triggering and guiding leader discharges using a plasma channel created by an ultrashort laser pulse," *Appl. Phys. Lett.* **76**, 819–821 (2000).
- A. Ionin, S. Kudryashov, A. Levchenko, L. Seleznev, A. Shutov, D. Sinitsyn, I. Smetanin, N. Ustinovsky, and V. Zvorykin, "Triggering and guiding electric discharge by a train of ultraviolet picosecond pulses combined with a long ultraviolet pulse," *Appl. Phys. Lett.* **100**, 104105 (2012).
- F. Theberge, J.-F. Daigle, J.-C. Kieffer, F. Vidal, and M. Châteauneuf, "Laser-guided energetic discharges over large air gaps by electric-field enhanced plasma filaments," *Sci. Rep.* **7**, 40063 (2017).
- A. Schmitt-Sody, J. Elle, A. Lucero, M. Domonkos, A. Ting, and V. Hasson, "Dependence of single-shot pulse durations on near-infrared filamentation-guided breakdown in air," *AIP Adv.* **7**, 035018 (2017).
- T.-J. Wang, J. Zhang, Z. Zhu, Y. Liu, N. Chen, H. Guo, H. Sun, Y. Leng, S. L. Chin, and R. Li, "Femtosecond laser filament guided negative coronas," *AIP Adv.* **10**, 035128 (2020).
- O. G. Kosareva, D. V. Mokrousova, N. A. Panov, I. A. Nikolaeva, D. E. Shipilo, E. V. Mitina, A. V. Koribut, G. E. Rizaev, A. Couairon, A. Houard, A. B. Savel'ev, L. V. Seleznev, A. A. Ionin, and S. L. Chin, "Remote triggering of air-gap discharge by a femtosecond laser filament and postfilament at distances up to 80 m," *Appl. Phys. Lett.* **119**, 041103 (2021).
- A. Houard, V. Jukna, G. Point, Y.-B. André, S. Klingebiel, M. Schultze, K. Michel, T. Metzger, and A. Mysyrowicz, "Study of filamentation with a high power high repetition rate ps laser at 1.03 μ m," *Opt. Express* **24**, 7437 (2016).
- T. Produit, P. Walch, C. Herkommer, A. Mostajabi, M. Moret, U. Andral, A. Sunjerga, M. Azadifar, Y.-B. André, B. Mahieu, W. Haas, B. Esmiller, G. Fournier, P. Krötz, T. Metzger, K. Michel, A. Mysyrowicz, M. Rubinstein, F. Rachidi, J. Kasparian, J.-P. Wolf, and A. Houard, "The laser lightning rod project," *Eur. Phys. J. Appl. Phys.* **93**, 10504 (2021).
- J. K. Wahlstrand, N. Jhaji, and H. M. Milchberg, "Controlling femtosecond filament propagation using externally driven gas motion," *Opt. Lett.* **44**, 199 (2019).
- A. A. Ionin, S. I. Kudryashov, D. V. Mokrousova, L. V. Seleznev, D. V. Sinitsyn, and E. S. Sunchugasheva, "Plasma channels under filamentation of infrared and ultraviolet double femtosecond laser pulses," *Laser Phys. Lett.* **11**, 016002 (2014).
- A. D. Koulouklidis, C. Lanara, C. Daskalaki, V. Y. Fedorov, and S. Tzortzakos, "Impact of gas dynamics on laser filamentation thz sources at high repetition rates," *Optic Lett.* **45**, 6835 (2020).
- A. Higginson, Y. Wang, H. Chi, A. Goffin, I. Larkin, H. M. Milchberg, and J. J. Rocca, "Wake dynamics of air filaments generated by high energy picosecond laser pulses at 1 kHz repetition rate," *Opt. Lett.* **46**, 5449 (2021).
- G. Point, C. Milián, A. Couairon, A. Mysyrowicz, and A. Houard, "Generation of long-lived underdense channels using femtosecond filamentation in air," *J. Phys. B* **48**, 094009 (2015).
- The Engineering ToolBox, "Air-thermal diffusivity," 2018.
- F. Vidal, D. Comtois, C.-Y. Chen, A. Desparois, B. L. Fontaine, T. W. Johnson, J.-C. Kieffer, H. P. Mercure, H. Pepin, and F. A. Rizk, "Modeling the triggering of streamers in air by ultrashort laser pulses," *IEEE Trans. Plasma Sci.* **28**, 418 (2000).
- S. Tzortzakos, B. Prade, M. Franco, A. Mysyrowicz, S. Huller, and P. Mora, "Femtosecond laser-guided electric discharge in air," *Phys. Rev. E* **64**, 57401 (2001).
- E. Schubert, D. Mongin, J. Kasparian, and J.-P. Wolf, "Remote electrical arc suppression by laser filamentation," *Opt. Express* **23**, 28640 (2015).
- B. Zhou, S. Akturk, B. Prade, Y.-B. André, A. Houard, Y. Liu, M. Franco, C. D'Amico, E. Salmon, Z.-Q. Hao, N. Lascoux, and A. Mysyrowicz, "Revival of femtosecond laser plasma filaments in air by a nanosecond laser," *Opt. Express* **17**, 11450–11456 (2009).
- L. Arantchouk, G. Point, Y. Brelet, B. Prade, J. Carbonnel, Y.-B. André, A. Mysyrowicz, and A. Houard, "Large scale tesla coil guided discharges initiated by femtosecond laser filamentation in air," *J. Appl. Phys.* **116**, 013303 (2014).
- The breakdown voltage measurement were made in a closed space. thus preventing the natural convection of air and fostering the apparition of cumulative effect. This could explained the presence of cumulative effect already at

10 Hz, despite not been visible at such repetition rate during previous experiments.

²⁴D. Comtois, H. Pépin, F. Vidal, F. A. M. Rizk, C.-Y. Chien, T. W. Johnston, J.-C. Kieffer, B. L. Fontaine, F. Martin, C. Potvin, P. Couture, H. P. Mercure, A. Bondiou-Clergerie, P. Lalande, and I. Gallimberti, "Triggering and guiding of

an upward positive leader from a ground rod with an ultrashort laser pulse-II: Modeling," *IEEE Trans. Plasma Sci.* **31**, 387 (2003).

²⁵E. M. Bazelyan and Y. P. Raizer, "The mechanism of lightning attraction and the problem of lightning initiation by lasers," *Phys.-Usp.* **43**, 701–716 (2000).